University of Nevada, Reno

Smart Meter Data-Driven Fault Location Algorithm in Distribution Systems

A thesis submitted in partial fulfillment of the requirements for the degree of Master of Science in Electrical Engineering

by

Kriti Dawadi

Dr. Hanif Livani/Thesis Advisor

May, 2016

THE GRADUATE SCHOOL

We recommend that the thesis
prepared under our supervision by

KRITI DAWADI

entitled

Smart Meter Data-Driven Fault Location Algorithm In Distribution Systems

be accepted in partial fulfillment of
the requirements for the degree of

MASTER OF SCIENCE

Hanif Livani, Ph.D., Advisor

M. Sami Fadali, Ph.D., Committee Member

Banmali Rawat, Ph.D., Committee Member

Thomas Quint, Ph.D., Graduate School Representative

David W. Zeh, Ph. D., Dean, Graduate School

May, 2016

ABSTRACT

Whenever there is a fault in the power system, the reliability of the network is compromised. This is why fault should be located as fast as possible and the system must be restored to the pre-fault values. Fault location and restoration is one of the functions of Distribution Automation (DA). In this thesis, we focus on faults in the distribution system. As distribution system is unbalanced, heterogeneous, and less voltage and current measurements are available, locating fault in the distribution system is more difficult than in the transmission system. Here, we propose a new algorithm that utilizes modern devices such as, smart meters, phasors measurement units (PMUs) and Fault Current Indicator (FIs).

The IEEE-123 bus system is used to demonstrate the proposed algorithm. Data from the smart meters and the PMUs were utilized for all the voltage and current measurements. The system is divided into eleven sections based on the status of FIs and circuit breakers (CBs). When a fault occurs, first the faulty section is identified. Then the fault resistance is estimated for all the buses in the faulty zone. Here, we find the fault resistance for each bus that will provide the same amount of current at the substation as the current measured during the fault. A flag is calculated from the measured and the simulated voltages at all the load buses. The proposed method can pinpoint the fault location precisely for any complex distribution system with load taps, laterals, single-phase loads, 3-phase loads, and heterogeneous lines. Four different cases are presented to test the proposed algorithm. Open Distribution System Simulator, along with Matlab, was used to demonstrate the performance of the proposed method.

ACKNOWLEDGEMENT

I feel honored to express my profound sense of gratitude and indebtedness to Dr. Hanif Livani, Department of Electrical and Biomedical Engineering, University of Nevada Reno, for his guidance, meticulous efforts, constructive criticism, inspiring encouragement, and unflinching and invaluable support as an advisor, which enabled me to enrich my knowledge and present it in this form.

I would like to extend my gratefulness to Dr. Sami Fadali and Dr. Thomas Quint for their perpetual encouragement, generous help, and inspiring guidance.

I want to thank Dr. Mehdi Etezadi-Amoli, and other faculty members in the Electrical and Biomedical Engineering department at University of Nevada, Reno.

I am also very thankful to the entire faculty and staff members of the Electrical and Biomedical Engineering Department for their help, co-operation, love, and affection.

I am very grateful to my family members, my parents, and my sweet little sister, for their encouragement and endless support. I don't think I would have made it without constant bugging of my sister.

Lastly, I would like to thanks Robert as well as all my friends from UNR who made my stay in UNR worthwhile and made this thesis possible.

Thank you.

CONTENTS

LIST OF TABLES

LIST OF FIGURES

LIST OF ACRONYMS

SCADA	Supervisory Control And Data Acquisition System
FI	Fault Current Indicator
CB	Circuit Breakers
DA	Distribution Automation
IED	Intelligent Electronic Device
R_f	Fault Resistance
AG	Phase A to ground fault
BG	Phase B to ground fault
LL	Line to line fault
LLG	Line-to-line-to-ground fault

CHAPTER 1

INTRODUCTION

Electric power systems consist of generators that generate power, a transmission and distribution system that delivers the power and the loads that consume the power, as shown in Figure. 1. The power in the transmission system is transmitted in high voltage (66kV to 765kV) in order to reduce the power loss. The voltage of the transmission system is stepped down in a substation to lower voltages (4kV to 25kV), which is further stepped down to 114-126 V (US standard) for end user utilization.

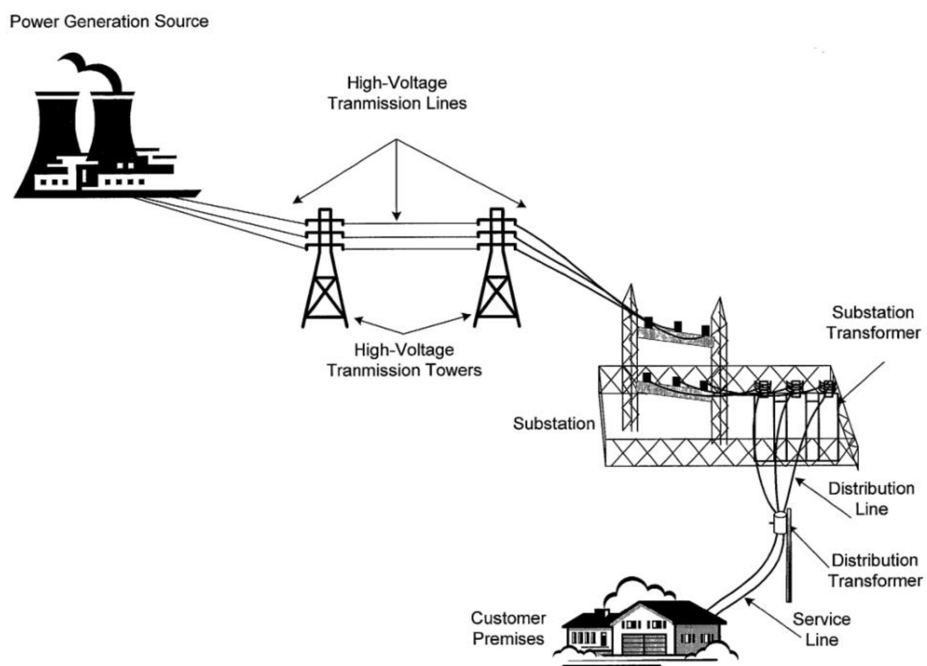

Figure 1. Power System from generation to distribution [51]

The delivery of electricity typically utilizes a supervisory control and data acquisition system (SCADA) that provides monitoring and control from generation through the step-down substation to detect the need for an increase/decrease in the generation. As society has become more dependent upon a reliable supply of electricity, the distribution system has emerged as one of the important links between the utility and consumer. One of the ways to have an efficient distribution network is by locating the faults quickly and restoring the system to pre-fault conditions. Fault location and restoration are one of the Distribution Automation (DA) functions which improves the reliability of the network, and is of prime importance to Utilities Company.

It is of utmost importance that electric power is delivered to the customer all the time. But for various reasons such as insulation breakdown, lightning, the breaking of a conductor, etc., a fault can occur in the system [25]. In an electric power system, a fault is any abnormal electric current. There are basically two types of faults: balanced and unbalanced. A symmetric or balanced fault affects all three phases equally. Roughly only 5% of the faults are symmetric. An asymmetric or unbalanced fault does not affect each of the three phases equally. Various types of asymmetric faults and their causes are:

- line-to-line - a short circuit between lines, caused by ionization of air, or when lines come into physical contact, for example due to a broken insulator.

- line-to-ground - a short circuit between one line and ground, very often caused by physical contact, for example due to lightning or other storm damage.

- double line-to-ground - two lines come into contact with the ground (and each other), also commonly due to storm damage.

1.1. Motivation

After the fault, the power supply at various locations can be lost, which means the reliability of the system is compromised. There is no way to completely eliminate faults, but it is possible to, at least, decrease the time needed to locate the fault and re-energizing the system.

Overhead power line faults can be the easiest to diagnose since the cause might be obvious, e.g., a tree has fallen across the line, or a utility pole is broken and the conductors are lying on the ground. Faults can be located in a cable system either with the circuits de-energized or energized. Fault location techniques can be broadly divided into terminal methods and tracer methods. Terminal methods use voltages and currents measured at the ends of the cable as in impedance-based methods. Tracer methods require inspection along the length of the cable [2]. Terminal methods can be used to locate the general area of the fault. In very simple wiring systems, the fault location is often found through inspection of the wires. In complex wiring system where the wires may be hidden, wiring faults are located with the travelling wave method. A reflectometer sends a pulse down the wire and then analyzes the returning reflected pulse to identify faults within the electrical wire.

Most prior work on fault location has been based on the impedance-based method or the travelling wave methods. Each of these methods has its own advantages and disadvantages. Here we propose a new method to locate a fault in the distribution system that is robust and fast.

1.2. Contribution

The contribution of this thesis is two-fold:

(i) Even though there are smart meters installed on many houses, a typical utility uses no more than 20 percent of the potential benefits of smart meter installation. Here, smart meters data is exploited for locating faults. This is also a step closer to realizing smart grids and Distribution Automation (DA).

(ii) The proposed method can accurately pinpoint a faulted bus for varied fault resistances, fault conditions, and loading conditions.

The proposed fault location algorithm is evaluated for the IEEE 123-bus system. The algorithm is tested for various test cases, including different locations, different fault resistance, different loading, etc. All the test case are simulated in Matlab and OpenDSS.

1.3. Thesis Organization

The thesis is structured as follows: Chapter 2 presents a literature review on different methods used for the fault location in distribution systems. Chapter 3 illustrates the proposed fault location method. In Chapter 4, different simulation scenarios are presented, based on the standard IEEE 123-bus system, to demonstrate the effectiveness of the proposed algorithm. The proposed fault location algorithm results are discussed. In Chapter 5, conclusion and future work are presented.

CHAPTER 2

LITERATURE REVIEW

2.1. Introduction

For low voltage and medium voltage power cables the basic failure modes are mainly conductor short circuits to ground, conductor to conductor short circuits, degraded insulation resistance or open circuits. Cable faults can be categorized into three main types, open conductor faults, shorted faults and high impedance faults. In this thesis, shorted faults will be covered. Considerable research and investigation have proceeded in the area of fault location and digital protection of transmission lines since the 1960's.

In this chapter, we review fault location techniques as well as possible future developments. The challenges faced in locating a fault in a distribution system will also be covered.

2.2. Fault Location in Distribution Grids

Unlike in the transmission systems, the distribution system is not homogenous and balanced. So, locating a fault in the distribution network is more challenging. The major obstacles in locating a fault in the distribution system are:

- There is a limited number of measurements along the path of the feeder. Usually, measurements are available only at the substation.
- Only a few Circuit Breaker (CB) and relay statuses are available, unlike the transmission system.

- The system is unbalanced.
- The load profile is changing throughout the day, so the measurements obtained during fault at a specific location are different at different times of a day.
- Line impedance is not uniformly distributed.
- The topology of the distribution system is diverse due to the presence of laterals, spurs, and single-phase taps.

Some of the traditional methods used to locate faults in distribution networks are:

2.2.1. Customer Call

This is the most traditional method of fault location. Whenever there is a fault in a system, a certain portion of the network might be de-energized. Customers who not getting power at their houses tend to call the utility company to let them know about the power-out. By knowing the customer's address, the utility company can narrow down the faulted area. Technician drive around the neighborhood searching for a pop-out fuse or broken line to locate the fault.

2.2.2. Impedance - Based Method

In this method voltage and current values measured at one or two ends of the lines are required. The apparent impedance is calculated based on the measured voltage and current. The distance of the fault from the primary distribution bus to the fault location can be estimated from the apparent impedance. Accurate fault location based upon impedance estimation depends on the accuracy of the calculated impedances.

The common method of calculation is based on equations developed by J.R. Carson, et al., in 1926 [57]. Another method of determining the line impedance parameters involves the direct measurement of the open circuit, and short circuit voltages and currents [7][21][37]. A third method involves the estimation of the line parameters through the solution of two-port equations based on synchronous phasor measurements obtained from direct measurements from a digital relay or a fault recorder [10][41].

One-ended impedance-based fault locators calculate the fault location from the apparent impedance seen looking into the line from one end while two-ended uses both the ends. To locate all fault types, the phase-to-ground voltages and currents in each phase must be measured. Impedance-based methods sometimes use source impedance data as well.

Consider a transmission line with two sources, as in Figure 2. There is a fault at distance 'm' from source G with fault resistance 'R_f'. I_G and I_H are the respective fault current from the two sources, G, and H.

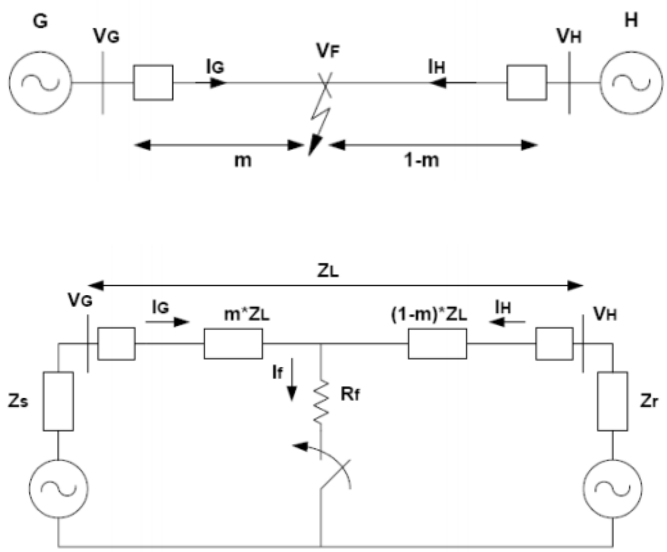

Figure 2. Simplified transmission line with two sources

Applying Kirchhoff's Voltage rule, we get:

$$V_G = m.Z_L.I_G + R_f.I_f \quad (2.1)$$

$$m = \frac{V_G - R_f.I_f}{Z_L.I_G} \quad (2.2)$$

$$= \frac{1}{Z_L}\left[\frac{V_G}{I_G} - R_f.\frac{I_f}{I_G}\right]$$

where, I_G = Line Current during fault

I_f = Fault current through the fault resistor R_f

Z_L = Impedance of the line

If fault resistance is assumed to be zero, we can use following calculation:

Table 1. Impedance based fault location calculation

Fault Type	Positive Sequence Impedance Equation ($m*Z_{IL}=$)
A - Ground	V_A / (I_A + k * 3* I_R)
B - Ground	V_B / (I_B + k * 3* I_R)
C - Ground	V_C / (I_C + k * 3* I_R)
A - B or A-B-G	V_{AB} / I_{AB}
B - C or B - C - G	V_{BC} / I_{BC}
C - A or C - A - G	V_{CA} / I_{CA}
A - B - C	Any of the following: V_{AB} / I_{AB} , V_{BC} / I_{BC} ,V_{CA} / I_{CA}

where,

$k = (Z_{OL} – Z_{IL})/(3 * Z_{IL})$
Z_{OL} = zero-sequence line impedance
Z_{IL} = positive sequence line impedance
m = per unit distance to fault
I_R: Residual Current

Impedance-based fault location is simple and economical, but has following disadvantages:

- It is not very accurate.
- It can give multiple estimate due to the multiple possible fault points at the same electrical distance from the measuring end [1].
- The source of error with the impedance methods of fault location has been identified as a phase shift between the current measured at one end of the line and that through the fault resistance [2].

2.2.3. Travelling Wave - Based Method

This method is based on the reflection and transmission of a fault generated traveling wave. The only inputs required to analyze fault data with the traveling wave fault locator are line length and wave velocity. The procedure is to energize the line in a radial fashion and then measure the time the reflected wave takes to return to the source. And, with help of wave velocity and time taken for reflection, distance to the fault is calculated. The known line length is compared with the length determined by the timing of the reflected wave.

There are two different travelling wave-based methods that are in use. One is to inject an electrical pulse into the faulted line segment and record the subsequently reflected signals (voltage and current) [2][13][14]. In [30], the travelling wave method is integrated with the complex matrix equations inherent in the mathematical model for three-phase systems, which were simplified by employing the concept of nodal analysis. The other approach is to record voltage and current at one or more points on an energized system within the first few milliseconds after fault inception. In both approaches fault location is estimated from the recorded data.

Travelling wave-based methods are more accurate than impedance-based method, but are expensive and need a high sampling rate of fault records.

2.2.4. Artificial Intelligence - Based Method

Several Artificial Intelligence (AI) based methods such as Artificial Neural Network (ANN), fuzzy logic, genetic algorithms, etc. are used to find the location of the fault. These methods substantially reduce the time factor and human error. AI methods require a data set for each type of fault. They use about 20% of that data to train the algorithm and the rest of the data is used to classify the faults [4][5]. To locate a fault, [31] uses a neural network, [32] uses a heuristics approach, [35] uses fuzzy logic.

2.2.5. Hybrid Method

The hybrid method is a combination of any of the previously described methods. For example, in [34] neural networks and fuzzy logic were implemented for the identification of animal-caused distribution faults. References [3], [4] and [5] have used a combination of a different method to locate faults in the system.

2.2.6. Modern Methods

The modern method of fault location use the modern devices such as smart meters, Phasors Measurement Unit (PMU), fault current indicators, etc to locate faults in transmission/distribution networks. Reference [45] uses synchronized voltage and current measurements at the interconnection of DG units, and [47] uses synchronized phasor measurement as its input. Using voltage and current phasor measurements at substations and/or feeder heads obtained through suitable communication schemes, candidate fault locations are identified by iterating every possible line segment in [48]. The main idea of [49] is to explore voltage measurements from monitors placed in different buses of distribution systems to estimate the fault location. A relationship matrix between possible fault locations (PFLs) and line currents (LCs) was derived in [50] and used to design an automatic and fast faulted line-section location method.

CHAPTER 3

FAULT LOCATION METHODOLOGY

3.1. Introduction

As distribution system can be huge (100-500 buses), locating a single fault by examining each bus is cumbersome and time-consuming. So, in this newly proposed method, a network will be divided into various sections/zones according to switches and Fault Current Indicators (FCIs). This will create smaller sections for analysis.

Locating a fault in a system usually reduces to determining the fault resistance R_f, as is the case in our method. Once the faulty zone is located, fault resistance for each of the buses in the faulted zone will be calculated by interpolating between simulated fault current and calculated fault current at the substation. The lowest flag value is then calculated to determine the two faulty buses.

We make the following assumptions:

- Fault type is known
- Pre-fault and fault voltage data from all the terminal ends are available
- Fault current at the substation is known
- Loading conditions are well-known

In this chapter, the proposed algorithm for fault location is formulated and explained in detail. Simulation results are provided in Chapter 4.

3.2. Smart Meter and Phasor Measurement Units

Smart meters and Phasor Measurement Units (PMUs) are the first steps towards preparing for the future smart-grid. A smart meter is an electronic device that records consumption of electric energy in intervals of an hour or less. It is installed by the utility company for collecting information related to consumers' energy consumption for monitoring and billing purposes. It is an advanced form of an automated meter reading (AMR), as it has other additional features. It can be used for power outage notification or to collect other end-user data, such as consumer-side voltage, current, active/reactive power, etc. Smart meters enable two-way communication between the meter and the central system. They can also collect data for remote monitoring.

Even though there are smart meters installed on many houses, a typical utility realizes no more than 20 percent of the potential benefits of smart meter and IED (Intelligent Electronics Device) installation [2]. An Intelligent Electronic Device (IED) is a microprocessor-based controller of power system equipment, such as circuit breakers, transformers, and capacitors banks.

Phasor Measurement Units (PMUs) or Synchrophasors are monitoring devices that measure accurately time-stamped voltages and currents phasors at critical locations on a power grid. They provide real-time measurement of electrical quantities across the power system with the help of a GPS clock. Unlike Supervisory Control and Data Acquisition (SCADA) that collect data every 2-10 seconds, PMUs can take 10-60 samples per second. The main achievement of PMUs is that as their measurements are synchronized, synchronized comparison of two quantities is possible in real time. PMUs are very expensive, which is why they are seen mostly in transmission systems.

Here, it is assumed that there are smart meters installed at all of the terminal ends and that voltage, current, and power data can be acquired from those devices. Also, there is one PMU installed at the substation, so that the substation can be monitored every second.

3.3. Fault Current Indicators (FIs)

Fault Current Indicators are devices which provide remote or visual indication of fault currents in electric power systems. When properly applied, they can reduce the outage time by properly identifying the section of the electric system that is faulted. During an electrical fault, additional current flows through a conductor and is picked up by the FIs causing a state change on LEDs or a remote indication device. The collected fault data are transmitted to DMS through a communication channel for further studies.

Figure 3 and 4 are examples of how fault indicators can be placed to assist line crews in fault location. Shown is a radial network with two branches. When a fault occurs in the system, it can either be upstream or downstream of the FIs. The FIs are triggered if the fault is upstream but not if it is downstream. For example, assume there is a fault between FI_6 and FI_7, FI_1, FI_2 and FI_6 are triggered while FI_3, FI_4, and FI_5 are not triggered. This indicates that the fault is upstream to FI_6, which gives the faulty region to be the second feeder as shown in Figure 3. If there is a fault in both feeders, FI_1, FI_2, FI_3, and FI_6 will be triggered. As FI_4 and FI_7 are not triggered, we will know that faulty section is between FI_3-FI_4 and FI_6-FI_7.

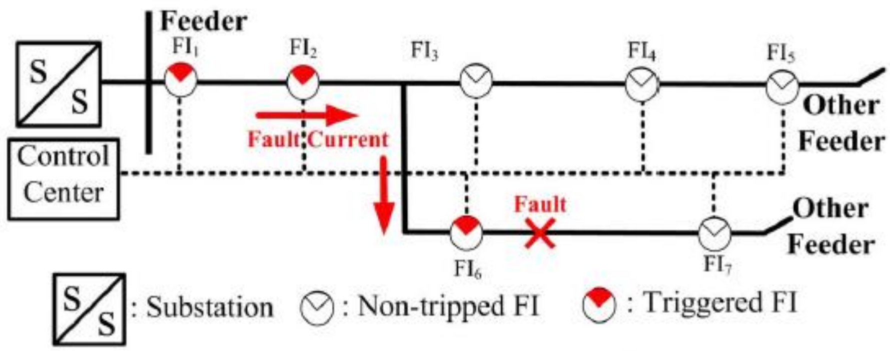

Figure 3. FIs in lateral network [43]

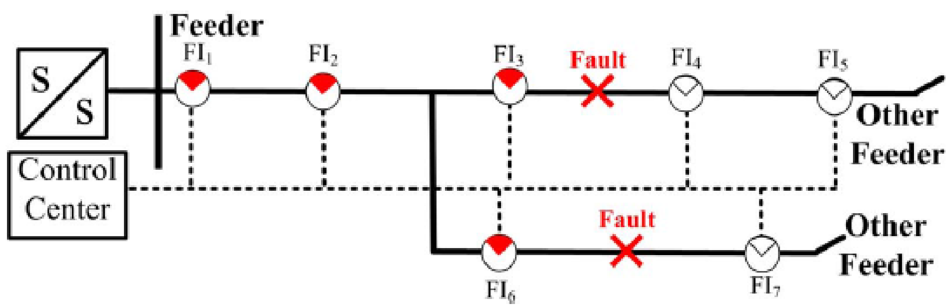

Figure 4. Locating faulty zone with help of FIs [43]

3.4. OpenDSS

OpenDSS is an electric power Distribution System Simulator (DSS) for supporting distributed resource integration and grid modernization efforts. It is a simulation tool, primarily for electric utility power distribution systems, that has been available since 1997. It supports nearly all frequency domain (sinusoidal steady-state) analyses commonly performed on electric utility power distribution systems. In addition, it supports many new types of analyses that are designed to meet future needs related to the smart grid, grid modernization, and renewable energy research. OpenDSS is designed to be indefinitely expandable so that it can be easily modified to meet future needs. Many IEEE Test Feeders have already been implemented in OpenDSS. For this thesis, the IEEE-123 bus system will be used in OpenDSS.

All of simulations presented in this thesis have been done in OpenDSS. OpenDSS was used for fault analysis and to obtain the simulated current and voltages at various nodes. Because OpenDSS does not have an inbuilt loop function, Matlab was integrated with OpenDSS for running all simulations. The code implemented in OpenDSS and Matlab is provided in the Appendix.

3.5. Estimation of the Fault Resistance

In order to locate a fault in the system, the fault resistance R_f is estimated. The fault resistance is only calculated for the nodes in a faulty section (as determined by the FCIs and CBs). Here, the fault resistance is estimated at a certain bus 'B' which will create the same fault current I_s as the current measured I_m during a fault at a substation. It can be shown that if the fault with $R_f = 0$ at a certain location cannot produce the same amount of current recorded at the substation, then for $R_f > 0$ it definitely cannot do so. This concept is used to eliminate some of the nodes.

The following procedure is carried out to calculate fault resistance:

- Step 1: A fault is applied at an assumed faulted node with $R_f = 0$ (Start from node 1 and add one node at a time until the last node is added).
- Step 2: The steady state fault current I_s at the substation is calculated using short circuit analysis in OpenDSS.
- Step 3: The calculated fault current I_s is compared with the measured fault current I_m at the substation.
  - If $I_s < I_m$, then the assumed node is eliminated and the next node is considered.
  - If $I_s > I_m$, the current node can be a candidate for the faulty node. The fault resistance (R_f) value is increased to 50 ohms in the next iteration, and fault analysis is performed again to get $I_s{}'$ at the substation. Then, fault resistance is estimated by extrapolating and interpolating between I_s and $I_s{}'$ as given by equation (3.1).

$$R_f = R_f + \left(R_f{}' - R_f\right) * \left(\frac{I_m - I_s}{Is' - I_s}\right) \qquad (3.1)$$

where,
R_f= Fault resistance at 0 ohm
$R_f{}'$= Fault resistance at 50 ohm
$I_m{}'$= Fault current measured at substation
I_s= Fault current at substation with $R_f = 0$
$I_s{}'$= Fault current at substation with $R_f = 50$

3.6. Flag calculation

After the fault resistance is estimated, three-phase voltage (V_s) is calculated at all the load buses by performing fault analysis in OpenDSS. Both the magnitude and angle of the voltages are taken into account during flag calculation. The polar form of magnitude and angle is converted into rectangular form of real and imaginary voltage, i.e,

$$V\theta = V_r + jV_i \tag{3.2}$$

The following equation is used for calculating the flag:

$$Flag = \sum_{k=1}^{95} \sum_{n=1}^{3} ((V_s^r - V_m^r)^2 + (V_s^i - V_m^i)^2) \tag{3.3}$$

where, V_s^r=simulated real voltage for estimated R_f
V_s^i=simulated imaginary voltage for estimated R_f
V_m^r=measured real voltage during fault
V_m^i=simulated real voltage during fault
n= 1,2,3 are the three phases of each node
k=1,2,....,95 are all the load buses where a smart meter is located

The flag is calculated for all the suspected faulty nodes. The node having the lowest flag value is the fault location.

3.7. Proposed Method

The proposed algorithm can be summarized in the following steps:

Step 1: Get all the terminal voltages V_m of the load buses from the smart meters and the current at the substation I_m from the PMU.

Step 2: Acquire the status of the FCIs and CBs, so that the fault region can be located. Get the bus number of all the nodes {i} in that faulty region.

Step 3: Put the fault at Bus{i} with $R_f = 0$ and calculate current at the substation (I_s).

- If $I_s < I_m$, move to next node and repeat Step 3.
- If $I_s > I_m$, the current node can be a candidate for the faulty node. Go to Step 4.

Step 4: Conduct short circuit analysis to calculate R_f using (3.1) and get all the terminal voltages (V_s)

Step 5: Calculate the Flag using (3.3). Go to next node and repeat Step 3 until you have calculated the flag for all of the nodes in the faulty region.

Step 6: Determine the two buses with lowest Flag values. The fault has occurred between those two nodes.

3.8. Flow Chart

The algorithm for the proposed method can be further simplified by the following flow chart in Figure. 5. First all the terminal voltages V_m of the load buses are acquired from the smart meters and the current at the substation I_m is retrieved from the PMU. Then, with the help of the FCIs and CBs, the fault region is located. From the faulty region, the bus nodes {i} are fetched. A fault at Bus{i} with $R_f = 0$ is simulated with OpenDSS and the current at the substation I_s is calculated. If the $I_s < I_m$, we move to the next node and the process is repeated simulating a fault with $R_f = 0$ for the new node. If $I_s > I_m$, the current node can be a candidate for the faulty node. Short circuit analysis is done to determine R_f using eq (3.1) and the terminal voltages (V_s) from all the load bus are acquired. Next, the flag is calculated using (3.3) for all the possible faulty nodes. The bus with the lowest flag value is the faulted bus.

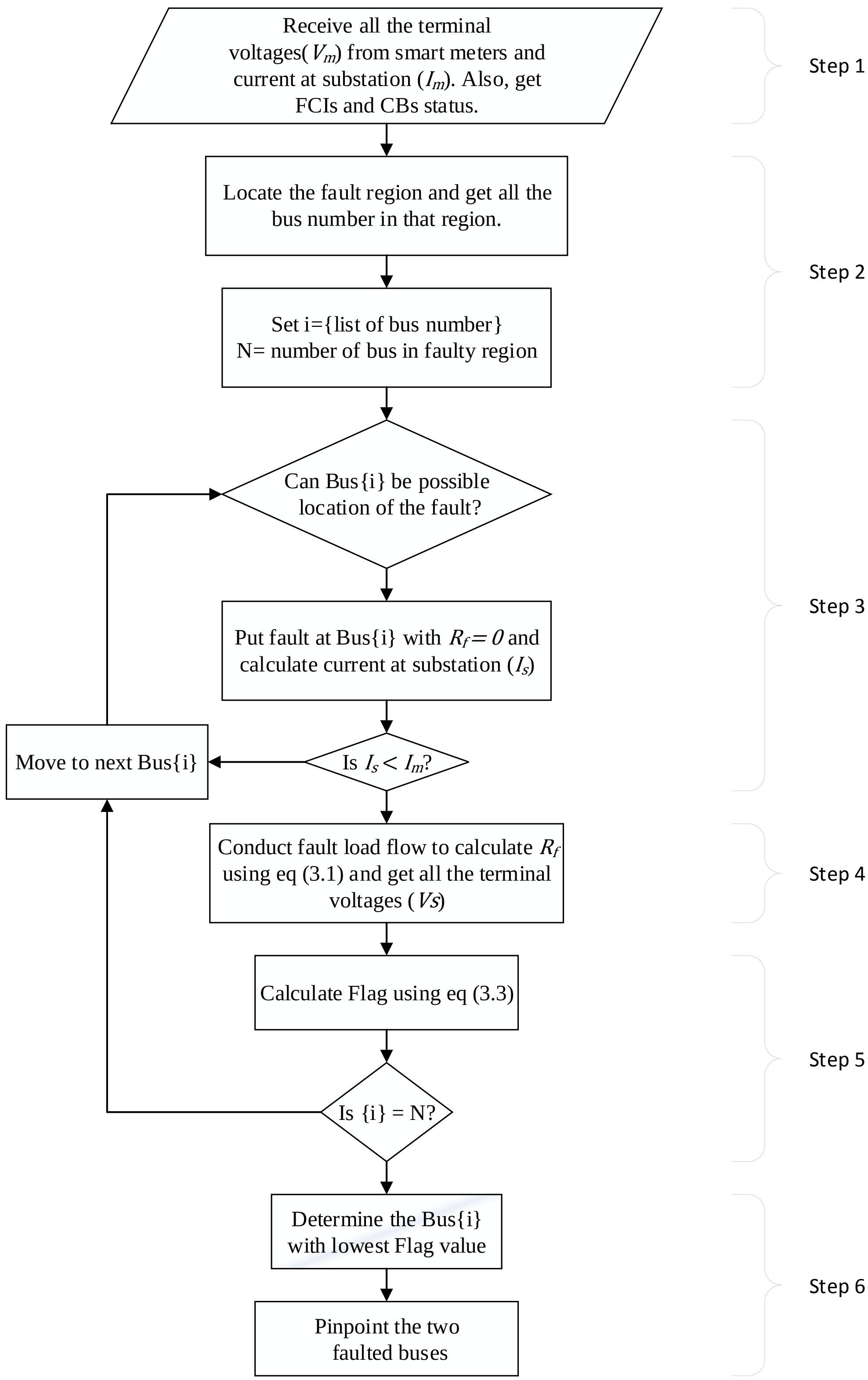

Figure 5. Flow chart for the proposed fault location algorithm

CHAPTER 4

SIMULATION RESULTS AND DISCUSSION

4.1. Introduction

In this chapter, the proposed fault location algorithm is evaluated on the IEEE 123-bus distribution system. Different case studies, including different fault resistances, different fault location, and various fault types test the robustness of the method.

4.2. The IEEE Standard Test Systems

4.2.1. The IEEE 123-bus system

The IEEE 123- bus system is a distribution system in which a 115kV system is stepped down at the substation to 4.16kV nominal voltage. This circuit has both overhead and underground lines. It is characterized by unbalanced loading with constant current, impedance, and power. There are four voltage regulators, four shunt capacitor banks, and eleven switches (five opened and six closed). This circuit has minimal convergence problems.

It is assumed that smart meters are placed at all the load buses, i.e. they are placed at all the buses except for 3, 8, 13, 14, 15, 21, 23, 25, 26, 27, 36, 40, 44, 54, 57, 61, 67, 72, 78, 81, 89, 91, 93, 97, 101, 105, 108 and 110. As PMUs are very expensive and not that common in the distribution systems, only one PMU is placed at the substation. The IEEE 123-bus system with all the smart meters and PMU is shown in Figure. 6.

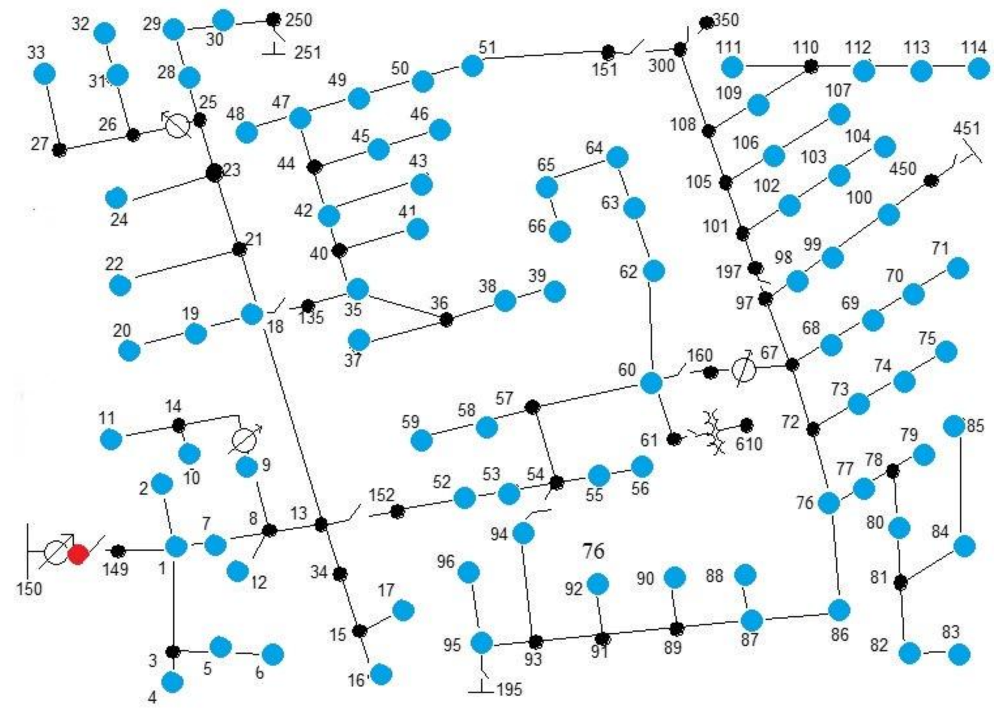

Figure 6. IEEE-123 bus system with all the smart meters and PMU

The closed switches are installed between nodes: 150-149, 13-152, 18-135, 60-160, 61-610, and 97-197. FCIs are placed at lines between nodes: 13-18, 23-25, 42-44, 76-86, 72-67, and 105-108. The network is divided into 11 regions based on the placement of FCIs and switches as shown in Figure 7.

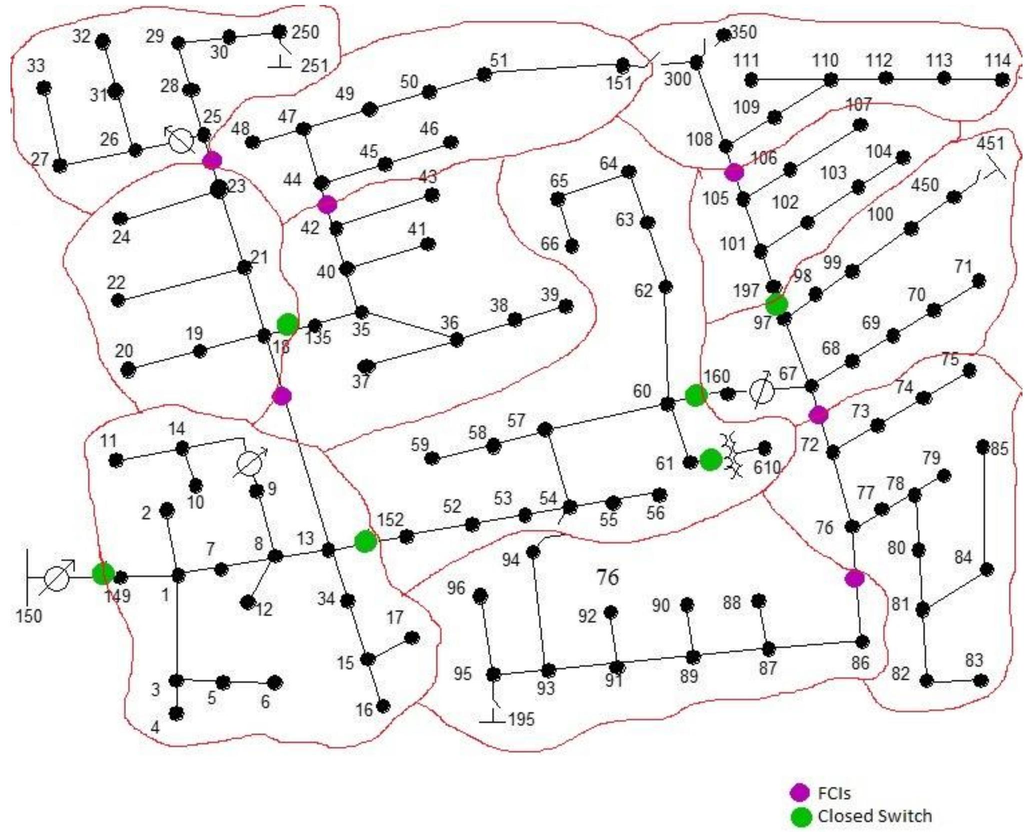

Figure 7. IEEE 123 bus system sectionalized with FIs

All the steady-state simulations were carried out using OpenDSS and Matlab. The built-in model of the IEEE-123 bus system was used for all the fault analysis. Gaussian noise is added to the measured voltages in all simulations to account for the impact of random errors. The noise is selected to have a zero mean and 0.01 standard deviation (σ).

4.3. Illustrative examples

The first example is of a LG fault, which illustrates how the proposed method works. An AG fault was created between nodes 21 and 23 with a fault resistance of 1Ω.

Step 1: Get all the terminal voltages V_m of the load buses from the smart meters and the current at the substation I_m from the PMU.

I_m=2510.75 A

Step 2: After acquiring the FCIs and CBs status, the fault region is found to be region-2. The buses that fall within faulty region are 18, 19, 20, 11, 22, 23, and 24.

Step 3: Put a fault at Bus 18 (19, 20 and so on) with $R_f = 0$ and calculate the current at the substation (I_s) (from OpenDSS). Bus 22 and 24 are eliminated as they don't have phase A. The I_s values are shown in Table 2.

Table 2. AG fault between buses 21 and 23

S.No.	Bus Number	I_s at $R_f = 0$	Comment
1.	18	6078.86	
2.	19	5175.23	
3.	20	4359.15	
4.	21	5343.56	
5.	22	X	Rejected (Phase B)
6.	23	4864.3	
7.	24	X	Rejected (Phase C)

Step 4: Estimate the fault resistance for all the buses where $I_s > I_m$ using (3.1). The terminal voltages V_S for the estimated R_f are simulated using OpenDSS. For this example, a fault resistance of 0.9115 at Bus 18 will create the same fault current (2510.75A) as measured during a fault. Different estimated fault resistances for possible faulted nodes are shown in Table 3.

Table 3. Fault resistance calculation for faulty section

S.No.	Bus Number	I_s at $R_f = 0$ (A)	$R_f(\Omega)$
1.	18	6078.86	0.9115
2.	19	5175.23	0.8215
3.	20	4359.15	0.6977
4.	21	5343.56	1.0210
5.	23	4864.3	0.9782

Step 5: The flag value is calculated for all the buses in the faulty region by using (3.3). The flag values are shown in Table 4.

Table 4. Flag calculation

S.No.	Bus Number	I_s at $R_f = 0$ (A)	$R_f(\Omega)$	Flag
1.	18	6078.86	0.9115	6.233×10^5
2.	19	5175.23	0.8215	7.87×10^5
3.	20	4359.15	0.6977	1.6×10^5
4.	21	5343.56	1.0210	5.45×10^4
5.	23	4864.3	0.9782	5.44×10^4

Step 6: A fault has occurred between the buses with the lowest flag values, as shown in Table 5. The faulted line is the line between bus 21 and bus 23 as identified by the proposed method.

Table 5. Determining faulty buses

S.No.	Bus Number	I_s at $R_f = 0$ (A)	$R_f(\Omega)$	Flag	Comment
1.	18	6078.86	0.9115	6.233×10^5	
2.	19	5175.23	0.8215	7.87×10^5	
3.	20	4359.15	0.6977	1.6×10^5	
4.	21	5343.56	1.0210	5.45×10^4	Lowest Flag
5.	23	4864.3	0.9782	5.44×10^4	Lowest Flag

4.3. Case Studies

Different fault scenarios under various system conditions (loading, fault type, R_f, and location) are simulated to evaluate the performance of the proposed method. The simulations are carried out for the following cases:

4.3.1. Different Fault resistance

Phase A to ground fault was simulated between nodes 21 and 23 for four different fault resistance; 0.1 ohms, 1 ohm, 5 ohms, and 10 ohms. With the help of FIs and CBs we isolated the faulty region, which contains node 18-24. The data for estimated R_f and flag value for all four resistances for possible faulty nodes are shown in Table 6. Bus 20 and 24 are ignored as they don't have phase A. We can see that the lowest flag value is for node 21 and 23 (the faulted node), for the four scenarios. For all the R_f values, the proposed method can locate the fault.

Table 6. Fault location for different fault resistances

S.No.	Bus Number	I_s at R_f=0	R_f=0.1, I_m=4750.64		R_f=1, I_m=2510.75		R_f=5, I_m=1125.18		R_f=10, I_m=840.387	
			R_f	Flag	R_f	Flag	R_f	Flag	R_f	Flag
1.	18	6078.86	0.1	6.24×10^6	0.9115	6.23×10^5	5.0398	2.748×10^4	10.058	7.278×10^3
2.	19	5175.23	0.1375	5.89×10^6	0.8215	7.87×10^5	4.9702	3.10×10^4	9.962	7.874×10^3
3.	20	4359.15			0.6977	1.6×10^5	4.887	3.928×10^4	9.8841	1.008×10^3
4.	**21**	**5343.56**	**0.110**	$\mathbf{4.08\times 10^5}$	**1.0210**	$\mathbf{5.45\times 10^4}$	**5.0119**	$\mathbf{2.64\times 10^3}$	**10.011**	**774.04**
5.	22	X								
6.	**23**	**4864.3**	**0.091**	$\mathbf{3.51\times 10^5}$	**0.9782**	$\mathbf{5.44\times 10^4}$	**4.988**	$\mathbf{2.24\times 10^3}$	**9.9899**	**681.4246**
7.	24	X								

4.3.2. Different Fault types

The proposed method is tested for various kinds of fault, such as LG, LL, LLG, and 3-phase.

1. AG fault:

Phase A to ground fault is created between 21 and 23, with fault resistance of 1 ohm. The current I_m at phase A of the source/substation is 2510.75 A during the fault. With the help of FIs and CBs we can isolate the faulty region, which contains node 18-24. The data for the estimated R_f and flag values for possible faulty nodes are shown in Table 7. Bus 22 and bus 24 are ignored as they do not have phase A. We can see that the lowest flag value is for node 21 and node 23 (the faulted node), as shown in Figure 8. For AG fault, the proposed method can locate the fault.

Table 7. Fault location for AG fault

S.No.	Bus Number	I_s at $R_f = 0$	R_f	Flag
1.	18	6078.86	0.9115	6.233×10^5
2.	19	5175.23	0.8215	7.87×10^5
3.	20	4359.15	0.6977	1.6×10^5
4.	**21**	**5343.56**	**1.0210**	$\mathbf{5.45\times 10^4}$
5.	22	X		
6.	**23**	**4864.3**	**0.9782**	$\mathbf{5.44\times 10^4}$
7.	24	X		

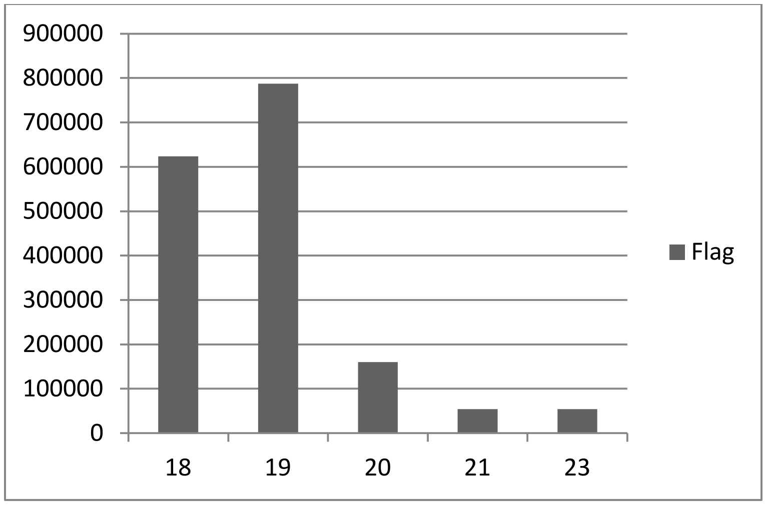

Figure 8. Flag value obtained for AG fault

2. BG fault

Phase B to ground fault is created between buses 106 and 107, with fault resistance of 5 ohms. The current I_m at phase B of the source/substation is 896.72 A during the fault. With the help of FIs and CBs, we can isolate the faulty region which contains node 101-107 and node 197. The data for the estimated R_f and flag values for possible faulty nodes are shown in Table 8. Bus 102, 103 and 104 are ignored as they don't have phase B. We can see that the lowest flag value is for node 106 and 107 (the faulted node), as shown in Figure 9. This shows that our method can locate a BG fault.

Table 8. Fault location for BG fault

S.No.	Bus Number	I_s at R_f =0	R_f	Flag
1.	197	3529.05	4.415	1.76×10^5
2.	101	3320.03	4.3844	1.76×10^5
3.	102	X		
4.	103	X		
5.	104	X		
6.	105	3119	4.351	1.841×10^5
7.	**106**	**2907.2**	**5.0868**	$\mathbf{6.246\times 10^3}$
8.	**107**	**2486.7**	**4.9118**	$\mathbf{4.570\times 10^3}$

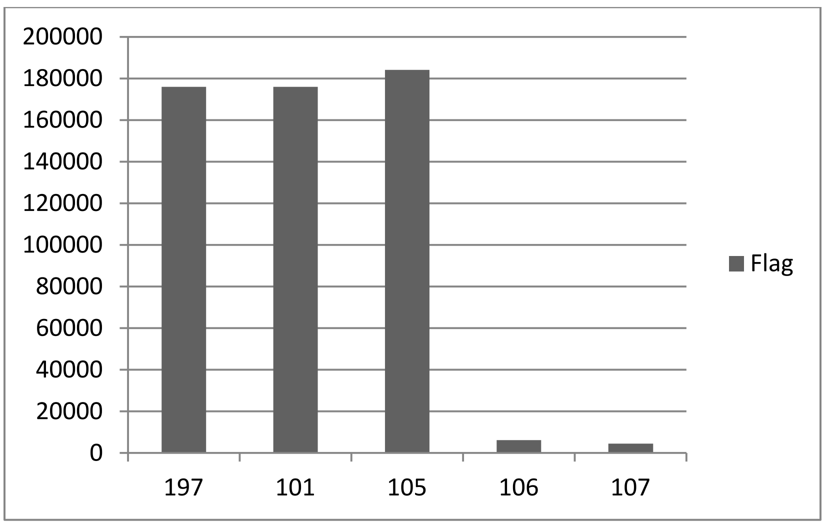

Figure 9. Flag value obtained for BG fault

3. LL

The line to line fault is created between bus 21 and 23, with fault resistance of 1 ohm. The fault is between phase A and phase B. The current (I_m) at phase A and phase B of the source/substation during the fault are 3654.7A and 3470.12A respectively. With the help of FIs and CBs we can isolate the faulty region that contains node 18-24. The data for estimated R_f and flag values for possible faulty nodes are shown in Table 9. Bus 19, 20, 22, and 24 are ignored because they have single phase line. We can see that the lowest flag value is for node 21 and 23 (the faulted node), as shown in Figure 10. For LL fault, the proposed method can locate the fault.

Table 9. Fault location for LL fault

S.No.	Bus Number	I_s at $R_f = 0$		R_f	Flag
1.	18	9173.4	8716.4	1.0786	7.69×10^5
2.	19	X	X		
3.	20	X	X		
4.	**21**	**8002.07**	**7533.13**	**1.0241**	$\mathbf{6.58\times 10^4}$
5.	22	X	X		
6.	**23**	**7246.1**	**6771.7**	**0.9751**	$\mathbf{6.05\times 10^4}$
7.	24	X	X		

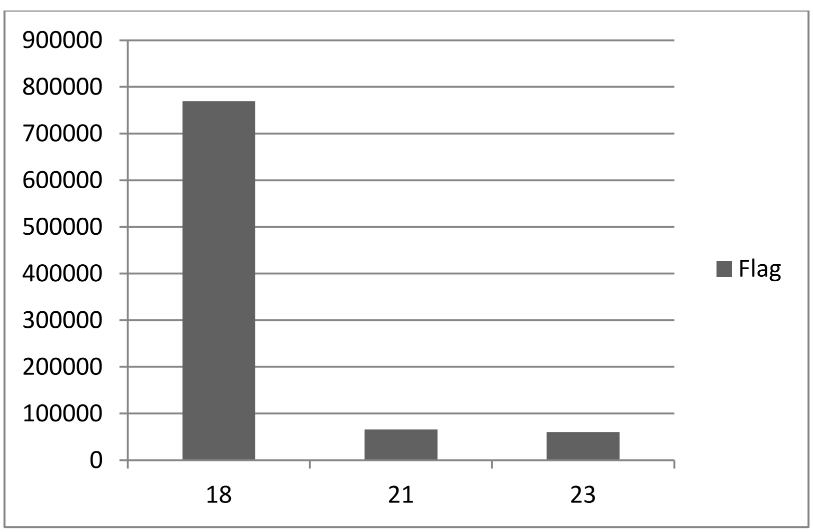

Figure 10. Flag value obtained for LL fault

4. LLG

A line-to-line-to-ground fault is created between bus 21 and bus 23, with fault resistance of 1 ohm. The fault is between phase A, phase B, and ground. The current at phase A and phase B of the source/substation during the fault are 2510.75A and 443.644A respectively. With the help of FIs and CBs, we can isolate the faulty region that contains node 18-24. The data for estimated R_f and flag values for possible faulty nodes are shown in Table 10. Buses 19, 20, 22, and 24 are ignored as they have single phase line. The lowest flag value is for node 21 and node 23 (the faulted node), as shown in Figure 11. For LLG fault, the proposed method can locate the fault.

Table 10. Fault Location for LLG fault

S.No.	Bus Number	I_s at $R_f = 0$		R_f	Flag
1.	18	6078.8	470.74	1.0688	5.75*$\times 10^5$
2.	19	X	X		
3.	20	X	X		
4.	21	**5343.56**	**463.81**	**1.0212**	**4.97$\times 10^4$**
5.	22	X	X		
6.	23	**4864.3**	**458.9**	**0.9784**	**4.75$\times 10^4$**
7.	24	X	X		

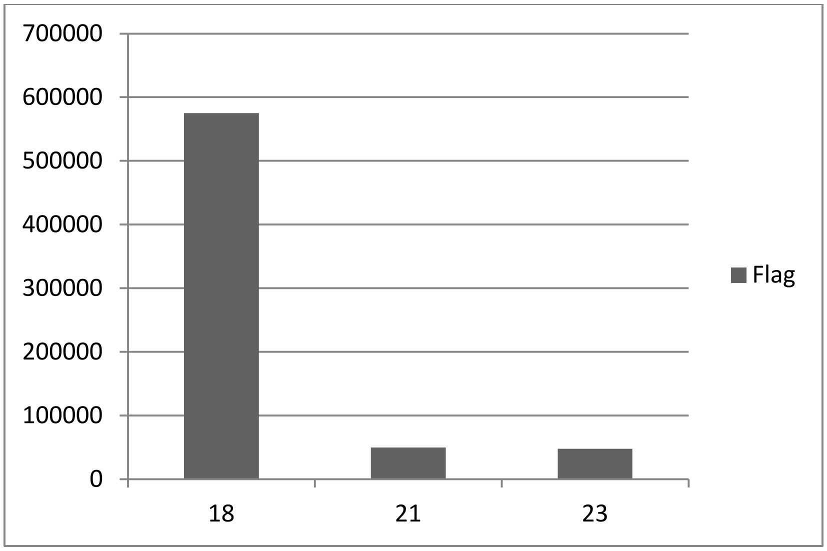

Figure 11. Flag value obtained for LLG fault

5. 3-phase fault

A 3-phase fault is created between bus 87 and bus 86, with fault resistance of 2.5 ohms. The fault is between phase A and phase B. The current at phase A, phase B and phase C of the source/substation during the fault are 1504A, 436.02A, and 519.07A respectively. With the help of FIs and CBs we can isolate the faulty region that contains nodes 86-94. The data for estimated R_f and flag values for possible faulty nodes are shown in Table 11. Buses 88, 90, 92, 94, and 96 are ignored as these are single phase line. We can see that the lowest flag value is for node 86 and 87 (the faulted node), as shown in Figure 12. For three phase fault, the proposed method can locate the fault.

Table 11. Fault location for three phase fault

S.No.	Bus Number	I_s at $R_f = 0$			R_f	Flag
1.	**86**	**2959**	**468**	**529**	**2.53**	$\mathbf{2.25\times 10^4}$
2.	**87**	**2745**	**464**	**527**	**2.4624**	$\mathbf{2.09\times 10^4}$
3.	88	X				
4.	89	2631	462	525	2.4151	8.94×10^4
5.	90	X				
6.	91	2547	460	525	2.3756	1.753×10^5
7.	92	X				
8.	93	2469	459	524	2.3346	2.756×10^5
9.	94	X				
10.	96	X				

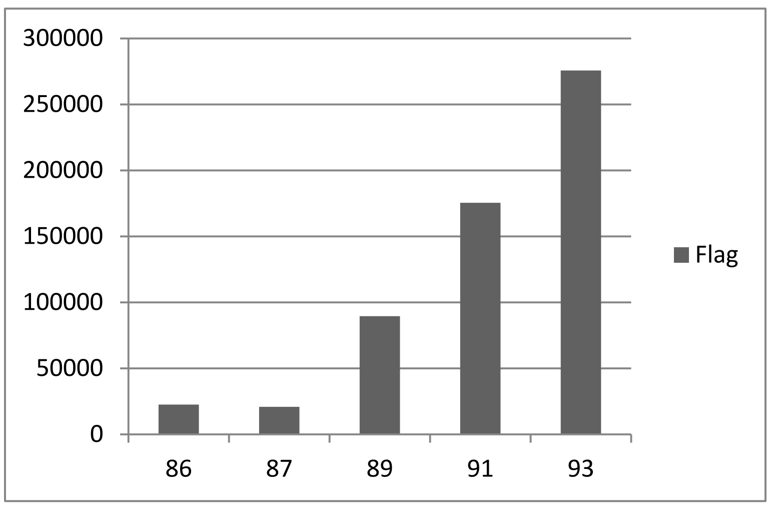

Figure 12. Flag value obtained for three phase fault

4.3.3. Different Loading Conditions

We simulated AG ground fault between buses 21 and 23 for three different loading conditions: 75%, 100%, and 125%. Fault resistance for all three conditions is 1 ohm. With the help of FIs and CBs, we can isolate the faulty region that contains nodes 18-24. The data for estimated R_f and flag values for possible faulty nodes are shown in

Table 12. As the loading of the system is increased, the current at the substation also increases. Buses 22 and 24 are ignored for all the three cases because they do not have the fault type considered. We can see that the lowest flag value is for node 21 and 23, the faulted node. For all the loading conditions, the proposed method can locate the fault accurately.

Table 12. Fault location for different loading conditions

S.No.	Loading	Bus Number	I_s at $R_f = 0$	R_f	Flag	Results
1.	75% I_m=2382A	18	6012.9	1.0722	5.99×10^5	
		19	5101.5	0.9832	5.02×10^5	
		20	4274.5	0.8622	7.06×10^5	
		21	**5273.7**	**1.0220**	$\mathbf{5.28\times 10^4}$	**Faulted**
		22	X			
		23	**4790.7**	**0.9773**	$\mathbf{5.06\times 10^4}$	**Faulted**
		24	X			
2.	100% I_m=2510A	18	6078.86	0.9115	6.233×10^5	
		19	5175.23	0.8215	7.87×10^5	
		20	4359.15	0.6977	1.6×10^5	
		21	**5343.56**	**1.0210**	$\mathbf{5.45\times 10^4}$	**Faulted**
		22	X			
		23	**4864.3**	**0.9782**	$\mathbf{5.44\times 10^4}$	**Faulted**
		24	X			
3.	125 % I_m=2819A	18	6726.49	1.0717	5.56×10^5	
		19	5735.63	0.9827	4.82×10^5	
		20	4843.16	0.8626	6.72×10^5	
		21	**5921.55**	**1.0219**	$\mathbf{4.84\times 10^4}$	**Faulted**
		22	X			
		23	**5897.37**	**0.9775**	$\mathbf{4.62\times 10^4}$	**Faulted**
		24	X			

4.3.4. Different Location

We divided the IEEE 123 bus system into eleven sections with the help of FIs and CBs. Here, we simulated eleven phase A to ground fault in those eleven different sections. We considered a fault resistance of 1 ohm for all the faults. With the help of FIs and CBs, the faulty region is isolated. The data for estimated R_f and flag values for possible faulty nodes are shown in Table 13. The fault condition is know, so the buses without phase A and buses with $I_s < I_m$ are ignored. The buses with "X" are the one without phase A. We can see that the lowest flag value is for the faulted node. For all the different location, the proposed method can locate the fault accurately.

Table 13. Different Locations

S.No.	**Location**	**Fault Type**	**Bus**	I_s	R_f	**Flag**	**Result**
1.	8-13 I_m=3204 A	AG	1	22012	1.118	1.187×10^7	
			2	X			
			3	X			
			4	X			
			5	X			
			6	X			
			7	18854.4	1.0655	3.65×10^6	
			8	14704.1	1.0282	7.709×10^5	**Faulted**
			9	10692.5	0.9601	8.112×10^5	
			10	6487.41	0.7371	2.97×10^6	
			11	6487.1	0.7366	2.98×10^6	
			12	X			
			13	11075.2	0.9709	7.44×10^5	**Faulted**
			34	X			
			15	X			
			16	X			
			17	X			

2.	27-33 I_m=2492A	AG	25	1930.5			
			26	3024.5	1.2529	1.01×10^6	
			27	3125.6	1.2021	5.38×10^5	**Faulted**
			28	621.1			
			29	621.2			
			30	621.1			
			31	X			
			32	X			
			33	3352.8	0.7762	5.16×10^5	**Faulted**
3.	49-50 I_m=2475A	AG	44	4536.31	1.126	7.30×10^5	
			45	4179.5	1.0502	4.99×10^5	
			46	3750.5	0.93	4.26×10^5	
			47	4231.5	1.0769	2.62×10^5	
			48	4069.8	1.0466	1.68×10^5	
			49	3969.85	1.0262	2.84×10^4	**Faulted**
			50	3742.8	0.973	2.86×10^4	**Faulted**
			51	3543.4	0.9158	2.31×10^5	
			151	3212.46	0.7892	1.22×10^6	
4.	36-37 I_m=2571A	AG	35	5742.9	1.17	1.02×10^6	
			36	4591.6	1.0582	6.23×10^4	**Faulted**
			37	4070.3	0.94	5.25×10^4	**Faulted**
			38	X			
			39	X			
			40	5236.0	1.125	8.16×10^5	
			41	X			
			42	4819.53	1.077	9.50×10^5	
			43	X			
5.	60-62 I_m=2540A	AG	52	8338.1	1.33	2.21×10^7	
			53	7434.3	1.29	1.90×10^7	
			54	6966.7	1.26	1.28×10^7	
			55	6130.9	1.22	1.20×10^7	
			56	5489.0	1.187	1.17×10^7	
			57	5948.1	1.203	1.05×10^7	
			58	X			
			59	X			
			60	4568.9	1.0455	6.31×10^4	**Faulted**
			61	3934.1	0.936	4.86×10^5	
			62	4224.5	0.954	5.35×10^4	**Faulted**
			63	4011.4	0.884	3.35×10^5	
			64	3645.82	0.757	1.12×10^6	
			65	3287.8	0.629	2.20×10^6	
			66	3067.7	0.463	4.32×10^6	

6.	89-91 I_m=2313A	AG	86	3344.7	1.21	1.70×10^6	
			87	3114.6	1.01	1.98×10^5	
			88	3002.4	1.02	1.22×10^5	
			89	2992.1	1.03	1.70×10^4	**Faulted**
			90	X			
			91	2900.7	0.9688	1.63×10^4	**Faulted**
			92	X			
			93	2861.0	0.9029	1.37×10^5	
			94	2683.3	0.7539	6.16×10^5	
			95	2712.4	0.809	4.40×10^5	
			96	X			
7.	77-78 I_m=2510A	AG	72	3954.08	1.146	1.26×10^6	
			73	X			
			74	X			
			75	X			
			76	3793.1	1.102	5.97×10^5	
			77	3511.4	1.012	8.10×10^4	**Faulted**
			78	3451.6	0.988	8.10×10^4	**Faulted**
			79	3322.8	0.93	1.72×10^5	
			80	3188.2	0.864	8.14×10^5	
			81	3103.1	0.814	1.47×10^6	
			82	2990.9	0.6425	4.43×10^6	
			83	2487.3			
			84	X			
8.	67-97 I_m=2683A	AG	67	4199.9	1.0271	6.79×10^4	**Faulted**
			68	3937.5	0.9429	1.24×10^5	
			69	3633.01	0.8224	8.13×10^5	
			70	3338.11	0.672	2.58×10^6	
			71	3130.25	0.534	4.98×10^6	
			97	3979.74	0.9724	6.82×10^4	**Faulted**
			98	3764.41	0.911	4.98×10^5	
			99	3407.04	0.7756	2.69×10^6	
			100	3244.24	0.6912	1.35×10^5	
9.	101-105 I_m=2569A	AG	101	3783.75			**Faulted**
			102	X			
			103	X			
			104	X			
			105	3591.01			**Faulted**
			106	X			
			107	X			
10.	113-114 I_m=1918A	AG	108	3307.3	1.69	2.74×10^6	
			109	2964.02	1.5027	1.30×10^7	
			110	2777.34	1.3732	6.99×10^5	

			111	2488.79	1.1186	5.89×10^5	
			112	277.56	1.3182	4.07×10^7	
			113	2455.84	1.077	1.59×10^5	**Faulted**
			114	2326.75	0.9199	1.12×10^5	**Faulted**
			300	2821.07	1.4919	2.68×10^6	
11.	21-23 I_m=2510A	AG	18	6078.86	0.9115	6.233×10^5	
			19	5175.23	0.8215	7.87×10^5	
			20	4359.15	0.6977	1.6×10^5	
			21	5343.56	1.0210	5.45×10^4	**Faulted**
			22	X			
			23	4864.3	0.9782	5.44×10^4	**Faulted**
			24	X			

4.5. Results and Discussions

The proposed fault location algorithm was tested for various fault scenarios. It was tested for different resistance values, loading conditions, and locations along the IEEE 123-bus system. We also simulated different kinds of faults such as AG, BG, LL, LLG, and 3-phase faults. The algorithm was robust and effective in locating the fault in all scenarios.

For all the different scenarios, the proposed algorithm was able to estimate the fault resistances. As shown in Table 6 to Table 13, the fault resistance estimated for the faulted node was the nearest to the true value. For other nodes, it was off by more than 10%. Let us take the example of AG fault between buses 21 and 23 again. We can see from Table 14 that for the faulted node the estimated resistance is off by only 2%.

Table 14. Percentage error in estimated $\boldsymbol{R_f}$

S.No.	Bus Number	I_s at $R_f = 0$	R_f	% error
1.	18	6078.86	0.9115	8.85%
2.	19	5175.23	0.8215	17.85%
3.	20	4359.15	0.6977	30.23%
4.	21	5343.56	1.0210	2.1%
5.	23	4864.3	0.9782	2.18%

The flag value for the faulted node was the lowest of all the conditions as seen from Table 9 to Table 13. The flag value for the faulted nodes was less than other nodes by a factor of 10-100 times. The nodes closer to faulted nodes had similar flag values as the faulted node. While the ones far from faulted nodes had larger flag value and can clearly be identified as not faulted.

CHAPTER 5

FUTURE WORK AND CONCLUSION

Different test cases of the IEEE 123-bus distribution systems were simulated to test the robustness of the proposed method. It was observed that for all the cases the proposed method can accurately pinpoint the faulted nodes.

In the past, a power generation station at one location would feed an entire load area. Nowadays we have a variety of power sources such as photovoltaic cells, diesel generator, fuel cell, etc. near the load area. This is known as Distributed Generation (DG). DG has many advantages. One of the main advantages of DG is that if a DG source is generating excess power, then we can send power back to the substation. This will help consumers decrease their utility bills. As DG causes a reversal of real power flows, it results in a significant power factor change. In addition, having a lot of DG in distribution network increase the probability of grid voltages exceeding allowable ranges. As a next step, we can include the distributed generation (DG) in the distribution system and observe how the proposed method of fault location work for DG injected system. We can repeat all the test cases for DG injected system.

For the future work, we will also evaluate the effectiveness and accuracy of the proposed algorithm in larger distribution grids such as the IEEE 342-bus and NVEnergy systems.

In this thesis, we used FIs and CBs to divide the distribution system into smaller sections. We can also examine clustering methods to divide the system into various sections.

5.1. Clustering (another method)

We can use k-means clustering technique to divide the system into zones, instead of using FIs. K-means is one of the simplest unsupervised learning algorithms that solve the well-known clustering problem. The main idea is to define 'k' centroids, one for each cluster. Given a set of observations (x1, x2, …, xn), where each observation is a d-dimensional real vector, k-means clustering aims to partition the n observations into k(≤ n). Its objective is to minimize the within-cluster sum of squares of distance functions of each point in the cluster to the K center.

We simulated AG fault in IEEE 123-bus system. We plotted the voltage (real and imaginary) from all the buses for phase A and use k-means clustering technique. We can increase the number of clusters as required. Here, the network was divided into four clusters as shown in figure 12. The cluster closest to the origin is the faulted cluster. So, in this case, red is the faulted cluster.

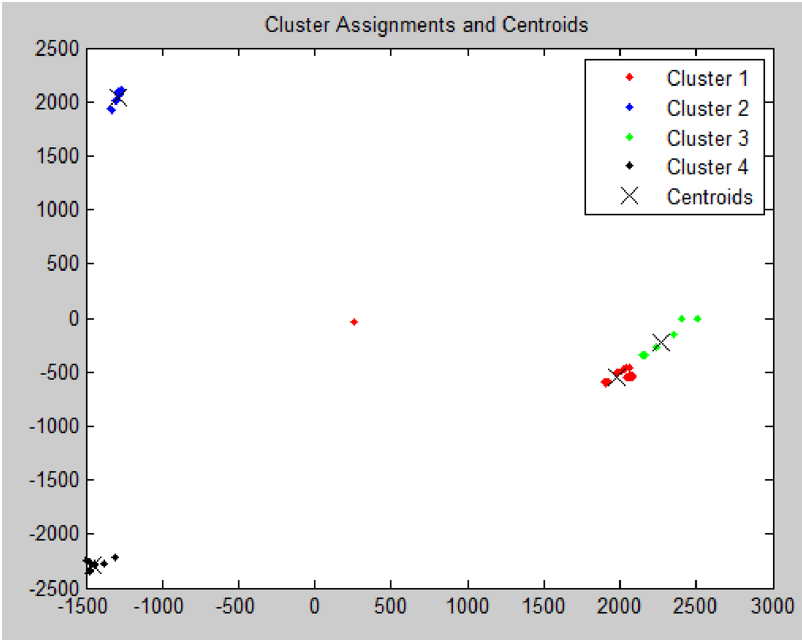

Figure 13. Clustering for IEEE 123 bus system for AG fault

REFERENCE

[1] Ramar Krishnathevar and Eng Eng Ngu, "Generalized Impedance-Based Fault Location For Distribution Systems"

[2] A. O. Ibe and B. J. Cory, "A Travelling Wave-Based Fault Locator For Two- And Three-Terminal Networks"

[3] Saeed Lotfifard, Mladen Kezunovic and Mirrasoul J. Mousavi," Voltage Sag Data Utilization For Distribution Fault Location"

[4] Hanif Livani, C. Yaman Evrenosoglu, Virgilio A. Centeno, " A Machine Learning-Based Faulty Line Identification for Smart Distribution Network"

[5] Hanif Livani, C. Yaman Evrenosoglu, "A Fault Classification and Localization Method for Three-Terminal Circuits Using Machine Learning"

[6] M. Jaya Bharata Reddy, D. Venkata Rajesh, Pathirikkat Gopakumar, and Dusmanta Kumar Mohanta, "Smart Fault Location for Smart Grid Operation Using RTUs and Computational Intelligence Techniques"

[7] Gustavo D. Ferreira, Daniel S. Gazzana, Arturo S. Bretas, and Afonso S. Netto, "A Unified Impedance-Based Fault Location Method for Generalized Distribution Systems"

[8] A. A. Girgis, D. G. Hart, W. L. Peterson, "A new fault location technique for two- and three-terminal lines"

[9] L. Eriksson, M. M. Saha, G. D. Rockefeller, "An Accurate Fault Locator With Compensation For Apparent Reactance In The Fault Resistance Resulting From Remore-End Infeed"

[10] Joe-Air Jiang ,Ying-Hong Lin , Jun-Zhe Yang , Tong-Ming Too , "An adaptive PMU based fault detection/location technique for transmission lines. II. PMU implementation and performance evaluation"

[11] A. A. Girgis ,C. M. Fallon , D. L. Lubkeman, "A fault location technique for rural distribution feeders"

[12] G. B. Ancell , N. C. Pahalawaththa, "Maximum likelihood estimation of fault location on transmission lines using travelling waves"

[13] P. Jafarian , M. Sanaye-Pasand, "A Traveling-Wave-Based Protection Technique Using Wavelet/PCA Analysis"

[14] R. H. Diaz and T. M. Lopez, "Fault location techniques for electrical Distribution networks: A literature survey," in Proc. 5th IASTED Int. Conf., Power and Energy Syst., Benalmadena, Spain, Jun. 15–17, 2005, Pp. 311–318.

[15] A. A. Girgis, C. M. Fallon, and D. L. Lubkeman, "A fault location Technique for rural distribution feeders," IEEE Trans. Ind. Appl., vol. 29, no. 6, pp. 1170–1175, Dec. 1993.

[16] J. Mora-Florez, J. Melendez, and G. Carrillo-Caicedo, "Comparison of impedance fault location methods for power distribution systems," Elect. Power Syst. Res., vol. 78, pp. 657–666, 2008.

[17] J. Mora-Florez, V. Barrera-Nuez, and G. Carrillo-Caicedo, "Fault location in power distribution systems using a learning algorithm for multivariable Data analysis," IEEE Trans. Power Del., vol. 22, no. 3, pp. 1715–1721, Jul. 2007

[18] Leif Eriksson, Murari Mohan Saha, G. D. Rockefeller, "An Accurate Fault Locator With Compensation For Apparent Reactance In The Fault Resistance Resulting From Remote-End Infeed"

[19] Hartstein Salim, Mariana Resener, André Darós Filomena, Karen Rezende Caino de Oliveira and Arturo Suman Bretas Rodrigo, "Extended Fault-Location Formulation for Power Distribution Systems"

[20] Gustavo D. Ferreira, Daniel S. Gazzana, Arturo S. Bretas, Member, IEEE, and Afonso S. Netto, "A Unified Impedance-Based Fault Location Method for Generalized Distribution Systems"

[21] Swagata Das, Surya Santoso, Anish Gaikwad, And Mahendra Patel, "Impedance-Based Fault Location in Transmission Networks: Theory and Application"

[22] Kongming Sun, Qing Chen, Zhanjun Gao, Dawei Liu, "Generalized Impedance-based Fault Distance Calculation Method for Power Distribution Systems"

[23] Energy and Environmental Economics, Inc., EPRI Solutions, Inc., "Value Of Distribution Automation Applications"

[24] Jiyuan Fan, Willem du Toit, Paul Bachsheider, "Distribution Substation Automation in Smart Grid"

[25] John McDonald, "Smart grid substation and feeder automation"

[26] W. L. Weeks, Sr. Member Ieee J. P. Steiner, Student Member IEEE, " Instrumentation For The Detection And Location Of Incipient Faults On Power Cables"

[27] Carlos H. Castro, Jennings B. Bunch, Terry M. Topka " Generalized Algorithms For Distribution Feeder Deployment And Sectionalizing Generalized Algorithms For Distribution Feeder Deployment And Sectionalizing"

[28] Curtis E. Taylor, " Fault Location On Rural Underground Power Lines"

[29] V. Cook, " Fundamental Aspects Of Fault Location Algorithms Used In Distance Protection"

[30] A.O. Ibe, B.J. Cory, " Fault-Location Algorithm For Multiphase Power Lines"

[31] Sonja Ebron David L. Lubkeman Mark White, " A Neural Network Approach To The Detection Of Incipient Faults On Power Distribution Feeders"

[32] Yuan-Yih Hsu, F. C. In, Y. Chien, J. P. Liu, J.T. Lm, H.S. Yu, R.T. Kuo, " An Expert System For Locating Distribution System Faults"

[33] Adly A. Girgis, Christopher M. Fallon, And David L. Lubkeman, " A Fault Location Technique For Rural Distribution Feeders"

[34] Mo-Yuen Chow, Yee, S.O., Taylor, L.S., " Recognizing Animal-Caused Faults In Power Distribution Systems Using Artificial Neural Networks"

[35] Jarventausta, P., Verho, P., Partanen, J., " Using Fuzzy Sets To Model The Uncertainty In The Fault Location Process Of Distribution Networks"

[36] Brahma, S.M., " Fault Location in Power Distribution System With Penetration of Distributed Generation"

[37] R.H. Salim, K.C.O. Salim, A.S. Bretas, " Further improvements on impedance-based fault location for power distribution systems"

[38] Das, S., Karnik, N., Santoso, S. " Distribution Fault-Locating Algorithms Using Current Only"

[39] Krishnathevar, R., Eng Eng Ngu, " Generalized Impedance-Based Fault Location for Distribution Systems"

[40] Ahmad Salehi-Dobakhshari, Ali Mohammad Ranjbar, " Application of synchronized phasor measurements to wide-area fault diagnosis and location"

[41] Ren, J., Venkata, S.S., Sortomme, E." An Accurate Synchrophasor Based Fault Location Method for Emerging Distribution Systems"

[42] Trindade, F.C.L., Freitas, W. ,Vieira, J.C.M., " Fault Location in Distribution Systems Based on Smart Feeder Meters"

[43] Jen-Hao Teng, Wei-Hao Huang, Shang-Wen Luan, " Automatic and Fast Faulted Line-Section Location Method for Distribution Systems Based on Fault Indicators"

[44] J. Barros, J.M. Drake, "Realtime Fault Detection And Classification In Power Systems Using Microprocessors"

[45] Brahma, S.M. , "Fault Location in Power Distribution System With Penetration of Distributed Generation"

[46] Das, S. , Karnik, N. , Santoso, S., "Distribution Fault-Locating Algorithms Using Current Only"

[47] Ahmad Salehi-Dobakhshari, Ali Mohammad Ranjbar, "Application of synchronized phasor measurements to wide-area fault diagnosis and location"

[48] Ren, J. , Venkata, S.S. , Sortomme, E., "An Accurate Synchrophasor Based Fault Location Method for Emerging Distribution Systems"

[49] Trindade, F.C.L. , Freitas, W. , Vieira, J.C.M., "Fault Location in Distribution Systems Based on Smart Feeder Meters"

[50] Jen-Hao Teng , Wei-Hao Huang , Shang-Wen Luan, "Automatic and Fast Faulted Line-Section Location Method for Distribution Systems Based on Fault Indicators"

[51] Facilitating communication of data signals on electric power systems, US 7053756 B2

[52] M.Majidi, M.Etezadi-Amoli, and M.S.Fadali, “A Novel Method for Single and Simultaneous Fault Location in Distribution Networks,” IEEE Transactions on Power System. Vol. 30, Issue 6, pp. 3368-3376, Nov. 2015.

[53] M.Majidi, A.Arabali, and M.Etezadi-Amoli, “Fault Location in Distribution Networks by Compressive Sensing,” IEEE Transactions on Power Delivery. Vol. 30, Issue 4, pp. 1761-1769, Aug. 2015.

[54] M.Majidi, M.Etezadi-Amoli, and M.S.Fadali, “A Sparse-Data- Driven Approach for Fault Location in Transmission Networks,” IEEE Transactions on Smart Grid.2015. Accepted for publication.

[55] M. Babakmehr, M.G. Simoes, M.B. Wakin, F. Harirchi. “Compressive Sensing-based Distributed Smart Grid Topology Identification” IEEE Transaction on Industrial Informatics 10.1109/TII.2016.2520396, 2016.

[56] M. Babakmehr, M. G. Simões, A. Al Durra, F. Harirchi, and Q. Han,“Application of compressive sensing for distributed and structured power line outage detection in smart grids,” in Proc. IEEE Amer. Control Conf. (ACC’15), Chicago, IL, USA, Jul. 2015, pp. 3682–3689.

[57] C37.114-2004 - IEEE Guide for Determining Fault Location on AC Transmission and Distribution Lines

APPENDIX

OpenDSS code

New object=circuit.ieee123

~ basekv=4.16 Bus1=150 pu=1.00 R1=0 X1=0.0001 R0=0 X0=0.0001

new transformer.reg1a phases=3 windings=2 buses=[150 150r] conns=[wye wye]

k_{VS}=[4.16 4.16] kvas=[5000 5000] XHL=.001 %LoadLoss=0.00001 ppm=0.0

new regcontrol.creg1a transformer=reg1a winding=2 vreg=120 band=2 ptratio=20

ctprim=700 R=3 X=7.5

! REDIRECT INPUT STREAM TO FILE CONTAINING DEFINITIONS OF

LINECODES

! This file defines the line impedances is a similar manner to the description in the test

case.

Redirect IEEELinecodes.DSS

! LINE DEFINITIONS

! Lines are defined by referring to a "linecode" that contains the impedances per unit

length

! So the only properties required are the LineCode name and Length

New Line.L1 Phases=1 Bus1=1.2 Bus2=2.2 LineCode=10 Length=0.175

New Line.L2 Phases=1 Bus1=1.3 Bus2=3.3 LineCode=11 Length=0.25

.....

New Line.L13a Phases=3 Bus1=13.1.2.3 Bus2=B1.1.2.3 LineCode=2

Length=0.4125

New Line.L13b Phases=3 Bus1=B1.1.2.3 Bus2=18.1.2.3 LineCode=2

Length=0.4125

....

New Line.L116 Phases=3 Bus1=152.1.2.3 Bus2=52.1.2.3 LineCode=1 Length=0.4

New Line.L117 Phases=3 Bus1=160r.1.2.3 Bus2=67.1.2.3 LineCode=6 Length=0.35

! NORMALLY CLOSED SWITCHES ARE DEFINED AS SHORT LINES

! Could also be defined by setting the Switch=Yes property

New Line.Sw1 phases=3 Bus1=150r Bus2=149 r1=1e-3 r0=1e-3 x1=0.000

x0=0.000 c1=0.000 c0=0.000 Length=0.001

! NORMALLY OPEN SWITCHES; DEFINED AS SHORT LINE TO OPEN BUS SO WE CAN SEE OPEN POINT VOLTAGES.

New Line.Sw7 phases=3 Bus1=151 Bus2=300_OPEN r1=1e-3 r0=1e-3 x1=0.000 x0=0.000 c1=0.000 c0=0.000 Length=0.001

! LOAD TRANSFORMER AT 61s/610

! This is a 150 kVA Delta-Delta stepdown from 4160V to 480V.

New Transformer.XFM1 Phases=3 Windings=2 Xhl=2.72

~ wdg=1 bus=61s conn=Delta kv=4.16 kva=150 %r=0.635

~ wdg=2 bus=610 conn=Delta kv=0.48 kva=150 %r=0.635

! CAPACITORS

! Capacitors are 2-terminal devices.

New Capacitor.C83 Bus1=83 Phases=3 kVAR=600 kV=4.16

New Capacitor.C88a Bus1=88.1 Phases=1 kVAR=50 kV=2.402

New Capacitor.C90b Bus1=90.2 Phases=1 kVAR=50 kV=2.402

New Capacitor.C92c Bus1=92.3 Phases=1 kVAR=50 kV=2.402

!REGULATORS

DEFINE TRANSFORMERS FOR REGULATORS

! Have to assume basically zero impedance regulators to match the test case

new transformer.reg2a phases=1 windings=2 buses=[9.1 9r.1] conns=[wye wye] k_{VS}=[2.402 2.402] kvas=[2000 2000] XHL=.01 %LoadLoss=0.00001 ppm=0.0

new transformer.reg3c like=reg3a buses=[25.3 25r.3] ppm=0.0

! SPOT LOADS

New Load.S1a Bus1=1.1 Phases=1 Conn=Wye Model=1 kV=2.4 kW=40.0 kvar=20.0

New Load.S2b Bus1=2.2 Phases=1 Conn=Wye Model=1 kV=2.4 kW=20.0 kvar=10.0

! Voltages are reported in per unit, so it is important to establish the base voltages at each bus

Set VoltageBases = [4.16, 0.48] ! ARRAY OF VOLTAGES IN KV

CalcVoltageBases ! PERFORMS ZERO LOAD POWER FLOW TO ESTIMATE VOLTAGE BASES

Solve !This will simulate steady state power flow

Show Voltage LN Nodes ! this shows the voltages by node, Line-to-Neutral voltage.

Show Currents Elements ! this produces a report of the currents, element-by-element.

```
Show Powers kva Elements  ! This produces a report of the powers, in kVA, element-by-element

!Simulating AG fault between Bus 13 and bus 18 with Rf=1 ohm

New Fault.F1 Bus1=B1.1 r=1

solve
show voltages
Export voltages  !Export LN voltages at all the buses as CSV file
```

MATLAB CODE

```
clc
clear all
close all
% **************************************************
% * Initialize OpenDSS
% **************************************************
% Instantiate the OpenDSS Object
DSSObj = actxserver('OpenDSSEngine.DSS');
% Start up the Solver
if ~DSSObj.Start(0),
disp('Unable to start the OpenDSS Engine')
return
end
% Set up the Text, Circuit, and Solution Interfaces
DSSText = DSSObj.Text;
DSSCircuit = DSSObj.ActiveCircuit;
DSSSolution = DSSCircuit.Solution;

%% Getting Isource at Rf=0
Is=2297.1;
Rf=0;
bus=23;
DSSText.Command = 'clear';
DSSText.Command = 'new circuit.ieee123 basekV=4.16 pu=1.000';
DSSText.Command = 'redirect
C:\OpenDSS\IEEETestCases\123Bus\Run_IEEE123Bus.DSS ';
```

```
DSSText.Command = 'redirect
C:\OpenDSS\IEEETestCases\123Bus\IEEE123Master.DSS ';
DSSText.Command = 'set voltagebases=[4.16 0.48]';
DSSText.Command = 'calcvoltagebases';
DSSText.Command = 'set controlmode=OFF';
DSSText.Command = ['New fault.F1    phases=1
bus1=',num2str(bus),'.1.2',' ','r=' ,num2str(Rf)];
%DSSText.Command = ['New fault.F1   phases=1 bus1=B2.1.2 r=1'];
DSSText.Command = 'solve';
DSSText.Command = 'Export Currents';

%Reading the CSV file for current
M =
importdata('C:\OpenDSS\IEEETestCases\123Bus\ieee123_EXP_CURRENTS.CSV');
I1=M.data(1,1)

%% Getting Isource at Rf=50
Rf=50;
DSSText.Command = 'clear';
DSSText.Command = 'new circuit.ieee123 basekV=4.16 pu=1.000';
DSSText.Command = 'redirect
C:\OpenDSS\IEEETestCases\123Bus\Run_IEEE123Bus.DSS ';
DSSText.Command = 'redirect
C:\OpenDSS\IEEETestCases\123Bus\IEEE123Master.DSS ';
DSSText.Command = 'set voltagebases=[4.16 0.48]';
DSSText.Command = 'calcvoltagebases';
DSSText.Command = 'set controlmode=OFF';
```

```
DSSText.Command = ['New fault.F1    phases=1
bus1=',num2str(bus),'.1.2',' ','r=' ,num2str(Rf)];
DSSText.Command = 'solve';
DSSText.Command = 'Export Currents';

%Reading the CSV file for current
M =
importdata('C:\OpenDSS\IEEETestCases\123Bus\ieee123_EXP_CURRENTS.CSV');
I2=M.data(1,1);
Rf2=50;

%% Comparing Rf and interpolating
%e= abs(Is-I1);
e= I1-Is;
if e<0
    disp('Move to another node')
else
        while e>0.0001
            Rf1=0;
            Rf= Rf1+(Rf2-Rf1)*((Is-I1)/(I2-I1))
            Rf2=Rf;
            DSSText.Command = 'clear';
            DSSText.Command = 'new circuit.ieee123 basekV=4.16
pu=1.000';
            DSSText.Command = 'redirect
C:\OpenDSS\IEEETestCases\123Bus\Run_IEEE123Bus.DSS ';
            DSSText.Command = 'redirect
C:\OpenDSS\IEEETestCases\123Bus\IEEE123Master.DSS ';
```

```
            DSSText.Command = 'set voltagebases=[4.16 0.48]';
            DSSText.Command = 'calcvoltagebases';
            DSSText.Command = 'set controlmode=OFF';
            DSSText.Command = ['New fault.F1    phases=1
bus1=',num2str(bus),'.1.2',' ','r=' ,num2str(Rf)];
            DSSText.Command = 'solve';
            DSSText.Command = 'Export Currents';
            M =
importdata('C:\OpenDSS\IEEETestCases\123Bus\ieee123_EXP_CURRENTS.CSV');
            I2=M.data(1,1);
            e= abs(Is-I2)
        end
end
```

DATA OF IEEE 123-BUS SYSTEM

Line Segment Data

Node A	Node B	Length (ft.)	Config.
1	2	175	10
1	3	250	11
1	7	300	1
3	4	200	11
3	5	325	11
5	6	250	11
7	8	200	1
8	12	225	10
8	9	225	9
8	13	300	1
9	14	425	9
13	34	150	11
13	18	825	2
14	11	250	9
14	10	250	9
15	16	375	11
15	17	350	11
18	19	250	9
18	21	300	2
19	20	325	9
21	22	525	10
21	23	250	2
23	24	550	11
23	25	275	2
25	26	350	7
25	28	200	2
26	27	275	7
26	31	225	11
27	33	500	9
28	29	300	2
29	30	350	2
30	250	200	2
31	32	300	11
34	15	100	11
35	36	650	8
35	40	250	1

36	37	300	9
36	38	250	10
38	39	325	10
40	41	325	11
40	42	250	1
42	43	500	10
42	44	200	1
44	45	200	9
44	47	250	1
45	46	300	9
47	48	150	4
47	49	250	4
49	50	250	4
50	51	250	4
51	151	500	4
52	53	200	1
53	54	125	1
54	55	275	1
54	57	350	3
55	56	275	1
57	58	250	10
57	60	750	3
58	59	250	10
60	61	550	5
60	62	250	12
62	63	175	12
63	64	350	12
64	65	425	12
65	66	325	12
67	68	200	9
67	72	275	3
67	97	250	3
68	69	275	9
69	70	325	9
70	71	275	9
72	73	275	11
72	76	200	3
73	74	350	11
74	75	400	11
76	77	400	6
76	86	700	3
77	78	100	6
78	79	225	6
78	80	475	6

80	81	475	6
81	82	250	6
89	90	225	10
89	91	225	6
91	92	300	11
91	93	225	6
93	94	275	9
93	95	300	6
95	96	200	10
97	98	275	3
98	99	550	3
99	100	300	3
100	450	800	3
101	102	225	11
101	105	275	3
102	103	325	11
103	104	700	11
105	106	225	10
105	108	325	3
106	107	575	10
108	109	450	9
108	300	1000	3
109	110	300	9
110	111	575	9
110	112	125	9
112	113	525	9
113	114	325	9
135	35	375	4
149	1	400	1
152	52	400	1
160	67	350	6
197	101	250	3

Table 15.Three Phase Switches

Node A	Node B	Normal
13	152	closed
18	135	closed
60	160	closed
61	610	closed
97	197	closed
150	149	closed
250	251	open
450	451	open
54	94	open
151	300	open
300	350	open

Table 16. Overhead Line Configurations (Config.)

Config.	Phasing	Phase Cond.	Neutral Cond.	Spacing
		ACSR	ACSR	ID
1	A B C N	336,400 26/7	4/0 6/1	500
2	C A B N	336,400 26/7	4/0 6/1	500
3	B C A N	336,400 26/7	4/0 6/1	500
4	C B A N	336,400 26/7	4/0 6/1	500
5	B A C N	336,400 26/7	4/0 6/1	500
6	A C B N	336,400 26/7	4/0 6/1	500
7	A C N	336,400 26/7	4/0 6/1	505
8	A B N	336,400 26/7	4/0 6/1	505
9	A N	1/0	1/0	510
10	B N	1/0	1/0	510
11	C N	1/0	1/0	510

Table 17. Shunt Capacitors

Node	Ph-A	Ph-B	Ph-C
	kVAr	kVAr	kVAr
83	200	200	200
88	50		
90		50	
92			50
Total	250	250	250

Table 18. Switches

Node A	Node B	Normal
13	152	closed
18	135	closed
60	160	closed
61	610	closed
97	197	closed
150	149	closed
250	251	open
450	451	open
54	94	open
151	300	open
300	350	open

Table 19. Transformer Data

	kVA	kV-high	kV-low	R - %	X - %
Substation	5,000	115 - D	4.16 Gr-W	1	8
XFM - 1	150	4.16 - D	.480 - D	1.27	2.72

Table 16. Underground Line Configuration (Config.)

Config.	Phasing	Cable	Spacing ID
12	A B C	1/0 AA, CN	515

Regulator Data

Regulator ID:	1		
Line Segment:	150 - 149		
Location:	150		
Phases:	A-B-C		
Connection:	3-Ph, Wye		
Monitoring Phase:	A		
Bandw idth:	2.0 volts		
PT Ratio:	20		
Primary CT Rating:	700		
Compensator:	Ph-A		
R - Setting:	3		
X - Setting:	7.5		
Voltage Level:	120		
Regulator ID:	2		
Line Segment:	9 - 14		
Location:	9		
Phases:	A		
Connection:	1-Ph, L-G		
Monitoring Phase:	A		
Bandw idth:	2.0 volts		
PT Ratio:	20		
Primary CT Rating:	50		
Compensator:	Ph-A		
R - Setting:	0.4		
X - Setting:	0.4		
Voltage Level:	120		

Regulator ID:	3		
Line Segment:	25 - 26		
Location:	25		
Phases:	A-C		
Connection:	2-Ph,L-G		
Monitoring Phase:	A & C		
Bandwidth:	1		
PT Ratio:	20		
Primary CT Rating:	50		
Compenator:	Ph-A	Ph-C	
R - Setting:	0.4	0.4	
X - Setting:	0.4	0.4	
Voltage Level:	120	120	
Regulator ID:	4		
Line Segment:	160 - 67		
Location:	160		
Phases:	A-B-C		
Connection:	3-Ph, LG		
Monitoring Phase:	A-B-C		
Bandwidth:	2		
PT Ratio:	20		
Primary CT Rating:	300		
Compensator:	Ph-A	Ph-B	Ph-C
R - Setting:	0.6	1.4	0.2
X - Setting:	1.3	2.6	1.4
Voltage Level:	124	124	124

Spot Loads

Node	Load	Ph-1	Ph-1	Ph-2	Ph-2	Ph-3	Ph-4
	Model	kW	kVAr	kW	kVAr	kW	kVAr
1	Y-PQ	40	20	0	0	0	0
2	Y-PQ	0	0	20	10	0	0
4	Y-PQ	0	0	0	0	40	20
5	Y-I	0	0	0	0	20	10
6	Y-Z	0	0	0	0	40	20
7	Y-PQ	20	10	0	0	0	0
9	Y-PQ	40	20	0	0	0	0
10	Y-I	20	10	0	0	0	0
11	Y-Z	40	20	0	0	0	0
12	Y-PQ	0	0	20	10	0	0
16	Y-PQ	0	0	0	0	40	20
17	Y-PQ	0	0	0	0	20	10
19	Y-PQ	40	20	0	0	0	0
20	Y-I	40	20	0	0	0	0
22	Y-Z	0	0	40	20	0	0
24	Y-PQ	0	0	0	0	40	20
28	Y-I	40	20	0	0	0	0
29	Y-Z	40	20	0	0	0	0
30	Y-PQ	0	0	0	0	40	20
31	Y-PQ	0	0	0	0	20	10
32	Y-PQ	0	0	0	0	20	10
33	Y-I	40	20	0	0	0	0
34	Y-Z	0	0	0	0	40	20
35	D-PQ	40	20	0	0	0	0
37	Y-Z	40	20	0	0	0	0
38	Y-I	0	0	20	10	0	0
39	Y-PQ	0	0	20	10	0	0
41	Y-PQ	0	0	0	0	20	10
42	Y-PQ	20	10	0	0	0	0
43	Y-Z	0	0	40	20	0	0
45	Y-I	20	10	0	0	0	0
46	Y-PQ	20	10	0	0	0	0
47	Y-I	35	25	35	25	35	25
48	Y-Z	70	50	70	50	70	50
49	Y-PQ	35	25	70	50	35	20
50	Y-PQ	0	0	0	0	40	20
51	Y-PQ	20	10	0	0	0	0
52	Y-PQ	40	20	0	0	0	0
53	Y-PQ	40	20	0	0	0	0
55	Y-Z	20	10	0	0	0	0
56	Y-PQ	0	0	20	10	0	0
58	Y-I	0	0	20	10	0	0
59	Y-PQ	0	0	20	10	0	0
60	Y-PQ	20	10	0	0	0	0
62	Y-Z	0	0	0	0	40	20
63	Y-PQ	40	20	0	0	0	0
64	Y-I	0	0	75	35	0	0
65	D-Z	35	25	35	25	70	50
66	Y-PQ	0	0	0	0	75	35
68	Y-PQ	20	10	0	0	0	0
69	Y-PQ	40	20	0	0	0	0
70	Y-PQ	20	10	0	0	0	0
71	Y-PQ	40	20	0	0	0	0
73	Y-PQ	0	0	0	0	40	20
74	Y-Z	0	0	0	0	40	20
75	Y-PQ	0	0	0	0	40	20
76	D-I	105	80	70	50	70	50
77	Y-PQ	0	0	40	20	0	0
79	Y-Z	40	20	0	0	0	0
80	Y-PQ	0	0	40	20	0	0
82	Y-PQ	40	20	0	0	0	0
83	Y-PQ	0	0	0	0	20	10
84	Y-PQ	0	0	0	0	20	10
85	Y-PQ	0	0	0	0	40	20
86	Y-PQ	0	0	20	10	0	0
87	Y-PQ	0	0	40	20	0	0
88	Y-PQ	40	20	0	0	0	0
90	Y-I	0	0	40	20	0	0
92	Y-PQ	0	0	0	0	40	20
94	Y-PQ	40	20	0	0	0	0
95	Y-PQ	0	0	20	10	0	0
96	Y-PQ	0	0	20	10	0	0
98	Y-PQ	40	20	0	0	0	0
99	Y-PQ	0	0	40	20	0	0
100	Y-Z	0	0	0	0	40	20
102	Y-PQ	0	0	0	0	20	10
103	Y-PQ	0	0	0	0	40	20
104	Y-PQ	0	0	0	0	40	20
106	Y-PQ	0	0	40	20	0	0
107	Y-PQ	0	0	40	20	0	0
109	Y-PQ	40	20	0	0	0	0
111	Y-PQ	20	10	0	0	0	0
112	Y-I	20	10	0	0	0	0
113	Y-Z	40	20	0	0	0	0
114	Y-PQ	20	10	0	0	0	0
Total		1420	775	915	515	1155	635